Characterization and Application of Nanomaterials 2024, 7(1), 4671.
https://doi.org/10.24294/can.v7i1.4671

Article

Influence of green synthesized aluminum oxide nanoparticle concentration on wear and coefficient of friction of vegetable oil-based lubricants

Stephen Yebosoko Tsado[1], Tijani Jimoh Oladejo[2], Uzoma Gregory Okoro[1], Daniel Ipilakyaa Tertsegha[3], Ibrahim Ogu Sadiq[1], Joseph Abutu[4], Emmanuel Ogo Onche[5], Antwi Afari Acheampong[6], Alhassan Sullaiman[6], Ebenezer Adu Kyeremeh[6], Sunday Albert Lawal[1,6,*]

[1] Department of Mechanical Engineering, Federal University of Technology Minna, Minna 920101, Nigeria
[2] Department of Chemistry, Federal University of Technology Minna, Minna 920101, Nigeria
[3] Department of Mechanical Engineering, Joseph Sarwuan Tarka University, Makurdi 970101, Nigeria
[4] Department of Mechanical Engineering, Taraba State University, Jalingo 660213, Nigeria
[5] Department of Mechanical Engineering, University of Abuja, Giri 900105, Nigeria
[6] Department of Mechanical Engineering, University of Mines and Technology Tarkwa, Tarkwa 000031, Ghana
*** Corresponding author:** Sunday Albert Lawal, lawalsunday@futminna.edu.ng

CITATION

Tsado SY, Oladejo TJ, Okoro UG, et al. Influence of green synthesized aluminum oxide nanoparticle concentration on wear and coefficient of friction of vegetable oil-based lubricants. Characterization and Application of Nanomaterials. 2024; 7(1): 4671.
https://doi.org/10.24294/can.v7i1.4671

ARTICLE INFO

Received: 18 February 2024
Accepted: 26 March 2024
Available online: 18 April 2024

COPYRIGHT

Copyright © 2024 by author(s). *Characterization and Application of Nanomaterials* is published by EnPress Publisher, LLC. This work is licensed under the Creative Commons Attribution (CC BY) license.
https://creativecommons.org/licenses/by/4.0/

Abstract: Green manufacturing is increasingly becoming popular, especially in lubricant manufacturing, as more environmentally friendly substitutes for mineral base oil and synthetic additives are being found among plant extracts and progress in methodologies for extraction and synthesis is being made. It has been observed that some of the important performance characteristics need enhancement, of which nanoparticle addition has been noted as one of the effective solutions. However, the concentration of the addictive that would optimised the performance characteristics of interest remains a contending area of research. The research was out to find how the concentration of green synthesized aluminum oxide nanoparticles in nano lubricants formed from selected vegetable oils influences friction and wear. A bottom-up green synthesis approach was adopted to synthesize aluminum oxide (Al_2O_3) from aluminum nitrate ($Al(NO_3)_3$) precursor in the presence of a plant-based reducing agent—*Ipomoea pes-caprae*. The synthesized Al_2O_3 nanoparticles were characterized using TEM and XRD and found to be mostly of spherical shape of sizes 44.73 nm. Al_2O_3 nanoparticles at different concentrations—0.1 wt%, 0.3 wt%, 0.5 wt%, 0.7 wt%, and 1.0 wt%—were used as additives to castor, jatropha, and palm kernel oils to formulate nano lubricants and tested alternately on a ball-on-aluminum (SAE 332) and low-carbon steel Disc Tribometer. All the vegetable-based oil nano lubricants showed a significant decrease in the coefficient of friction (CoF) and wear rate with Ball-on-(aluminum SAE 332) disc tribometer up to 0.5wt% of the nanoparticle: the best performances (e_{COF} = 92.29; e_{WR} = 79.53) came from Al_2O_3-castor oil nano lubricant and Al_2O_3-palm kernel oil; afterwards, they started to increase. However, the performance indices displayed irregular behaviour for both COF and Wear Rate (WR) when tested on a ball-on-low-carbon steel Disc Tribometer.

Keywords: nanoparticles; green synthesized; wear; coefficient of friction; lubricants

1. Introduction

In recent times, vegetable oils have been identified as a favorite substitute for mineral oils as base oils in lubricant formulations. This is because vegetable oils possess high biodegradability and lubricity and, hence, can return to nature upon consumption after their useful lives. This property of vegetable oils makes them environmentally friendly alternatives to mineral oil-based lubricants. Researchers have carried out studies using vegetable oils as the base oil for lubricants while using various nanoparticle additives to improve its tribological performance [1–3]. Vegetable oils comprise the chemical composition of molecules of triacylglycerol made up of esters derived from glycerol and long chains of polar fatty acids [4]. Other vegetable oils are also composed of esters of glycerin and long-chain fatty acids (triglycerides), which have molecular structure with three long-chain fatty acids attached at the hydroxyl groups via ester linkages [5]. The chemical structure of a typical vegetable oil is shown in **Figure 1**.

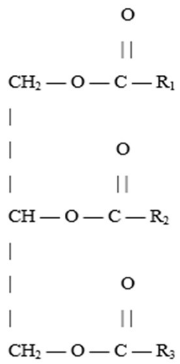

Figure 1. Chemical structure of triglyceride of a typical vegetable oil [5].

Other parameters that are determined through the process of formulating the oil-based lubricants are the acid value, saponification, and free fatty acid of the oil [6,7]. Nanoparticles ranging between 1 nm and 100 nm have all three external dimensions in the nanoscale, and their longest and shortest axes do not have a significant difference, typically being a factor of at least 3. Some examples are nonporous Pd NPs (0D), graphene nanosheets (2D), Ag nanorods (1D), polyethylene oxide nanofibers (1D), urchin-like ZnO nanowires (3D), and WO3 nanowire network (3D) [8]. Nanoparticles demonstrate desirable physical and optical characteristics such as shape and size, which makes them suitable to confine their electrons and produce quantum effects. These properties help in a complete description of its behavioural and operational functionalities, which deal with the size, shape, surface properties, crystallinity, and dispersion state [9]. The use of nanomaterials as additives to oil-base lubricants to produce nano lubricants with improved tribological properties has been gaining research attention in the industry in recent times [10]. This is essentially a result of their anti-wear, extreme pressure, and friction-modifying properties. Although there are different types of nanomaterials used in the formulation of nano lubricants, about 72% of nano lubricants are formulated using metal-containing nanomaterials as lubricant additives [11]. Among the various metallic nanoparticles that could be used as additives to lubricants, the Cu nanoparticles have received wide research attention for their superior performance in comparison with other metallic nanoparticles [12].

Metal nanoparticles are produced by the addition of reducing agents, while metal oxide nanoparticles are manufactured by the addition of oxidizing/precipitating agents during their synthesis [13]. Generally, when compared with metal-containing nanoparticles, the metal oxide nanoparticles are larger in size. Metal oxide nanoparticles have been shown to improve the viscosity of lubricants at low temperatures and the rolling effect of the lubricant at high temperatures, with deposition of the metal oxide nanoparticles on the interacting surfaces leading to improved anti-wear performance [11]. Utilizing metal oxide nanoparticles will improve the nano lubricant properties. These properties include the nanoparticle size, morphology/shape, surface functionalization, and nanoparticle concentration. In synthesizing the nanoparticles, the green synthesis method was used for this work. This is a bottom-up approach of the two methods of synthesizing. The other method, the top-down approach, emphasizes the preparation of nanoparticles from the process of breaking down complex metal ions through physical, chemical, or thermal methods [14], which is more costly to undertake.

Several nanoparticles have been used as additives to vegetable oils to investigate their effect on the tribological properties of lubricating oils. The major parameters varied are the size, shape, and concentration of the nanoparticles. Among other nanoparticles investigated, Al_2O_3 nanoparticles, a metal oxide nanoparticle, have the potency of improving the tribological performance of base oils. Also, most nanoparticles investigated are chemically synthesized, and this becomes a subject of interest and consideration when considering potential impacts on the environment on a large scale. Therefore, the investigation of the tribological performance of green synthesized Al_2O_3 nanoparticles as additives to vegetable oils for the development of nano lubricants as alternatives to mineral oil-based lubricants holds considerable potential in eco-friendly lubrication.

2. Materials and methods

The materials used in the study are vegetable oils, aluminum oxide (Al_2O_3) nanoparticles, aluminum nitrate ($Al(NO_3)_3$) salt, beach morning glory (stem) (*Ipomoea pes-caprae*), aluminum SAE 332 disc, low carbon steel disc, and distilled water. The vegetable oils are palm kernel oil (PKO), jatropha oil, and castor oil, and they were all locally sourced off the shelf. The aluminum oxide nanoparticles were synthesized based on the green synthesis method, as summarized in **Figure A1**. The Aqueous Leave Extract (ALE) was produced based on the hot extraction method as presented in **Figure 2**. This involves mixing a milled leaf in distilled water at a ratio 1 g to 20 mL in a beaker and heating the mixture to a temperature range of 60–80 °C for 1 h. The mixture is allowed to cool to room temperature and afterwards filtered using a Whatman-grade 540 filter paper. The ALE was further used in the synthesis of Al_2O_3 nanoparticles using a 0.1 M $Al(NO_3)_3$ solution as a precursor. The extracts were used to synthesize Al_2O_3 nanoparticles within 5 min of extraction. In synthesising the Al_2O_3 nanoparticles, an aqueous solution of 0.1 M $Al(NO_3)_3$ was prepared by dissolving 4.8286 g of the salt into 200 mL of distilled water. The mixture was stirred for 5 min at room temperature using the magnetic stirrer at a stirring speed of 300–320 rpm to ensure proper dissolution of all salt particles in the mixture. Using a ratio of 1:4 for the aqueous solution and plant extract, respectively, the plant extract was poured into the beaker with the stirring bar and placed on the magnetic stirrer. The temperature of the stirrer was set at 60 °C, and the speed was set at 320 rpm. UV-Visible adsorption spectra analysis was conducted to determine the wavelength and absorption of the synthesized mixture using the UV-Vis spectrophotometer. The result of the analysis gave the size distribution of the Al_2O_3 nanoparticles. Synthesized Al_2O_3 nanoparticles were further subjected to drying and calcination in order to obtain dried and powdered nanoparticles. The synthesized mixture was centrifuged at a rotational speed of 8000 rpm to remove excess moisture content and impurities that may be less dense compared to the precipitate using a high-speed refrigerated centrifuge. The resulting mixture was further subjected to freeze drying using a freeze dryer. The freeze dryer removed moisture content and produced the powdered Al_2O_3 nanoparticles. Furthermore, in order to get rid of residual moisture content and impurities, the dried nanoparticles were calcined at a temperature of 700 °C for 1 h using an electric oven.

Figure 2. Plant extraction process.

The characterization of the Al_2O_3 nanoparticles was done based on transmission electron microscopy (TEM) to determine the particle size distribution and morphology of the synthesized Al_2O_3 nanoparticles and X-ray diffraction analysis (XRD) to determine the structure of the synthesized Al_2O_3 nanoparticles. Vegetable oils comprising of palm kernel oil, jatropha oil, and castor oils at 0 wt% concentration of nanoparticles were characterised to serve as control experiments of the vegetable oils before addition of the nanoparticles. The properties examined are dynamic viscosity @24 °C (mPa/s), dynamic viscosity @40 °C, dynamic viscosity @100 °C, kinematic viscosity @40 °C (m^2/s), kinematic viscosity @100 °C, density (g/cm^3), specific gravity, flash point (°C), fire point (°C), pour point (°C), cloud point, smoke point, acid value (KOH/g), saponification (KOH/g), and free fatty acids (FFA). The oils were tested using a rotor labeled "3" at a rotational speed of 60 rpm. To determine the smoke point, flash point, and fire point, a volume of the oil sample was poured into a 5 mL crucible, placed on a heating element, and temperatures were taken at smoke, flash, and fire conditions. Furthermore, cloud and pour points were determined using a freezer with temperatures taken at cloud and pour conditions. The acid value, saponification, and free fatty acid of the oils were determined by the use of 25 mol of methanol that was prepared, and n-hexane was added in a ratio of 1:1.

The study adopted the two-step method in the preparation of the lubricants. The nanoparticles synthesized and characterized were dispersed into the base oil. The base vegetable oils used are palm kernel oil (PKO), jatropha oil (JO), and castor oil (CO). 50 g of nano lubricants were prepared by dispersing dry powder nanoparticles of size 44.73 nm at concentrations of 0.1 wt%, 0.3 wt%, 0.5 wt%, 0.7 wt%, and 1.0 wt% into the vegetable oils as shown in **Table 1**. The mixture was stirred for 10 min at a speed of 300–320 rpm and a stirring temperature of 60–80 °C using a magnetic stirrer. The nanoparticles were weighed using a chemical weighing balance. A total of 18 samples were prepared, including control samples.

Table 1. Mixture ratio for preparation of nano lubricants.

Nanoparticle concentration (g)	PKO (g)	JO (g)	CO (g)
0	50	50	50
0.05	49.95	49.95	49.95
0.15	49.85	49.85	49.85
0.25	49.75	49.75	49.75
0.35	49.65	49.65	49.65
0.5	49.5	49.5	49.5

The concentration was computed using the Equation (1).

$$\text{Mass (wt\%)} = \frac{\text{Mass of solute (NPs)}}{\text{Mass of solution (Oil + NPs)}} \times 100\% \tag{1}$$

The tribological test for the formulated nano lubricants was done using a ball-on-disc tribometer to determine the coefficient of friction (COF) and wear rate of the nano lubricants formulated. The parameters for the tribological tests used are shown in **Table 2**. A total of 38 metal disc samples of 30 mm diameter each were prepared from aluminum (SAE 332) and low-carbon steel. The samples were cast from the waste piston and engine block. They were further machined into discs of 30 mm diameter, polished, and etched to improve the surface finishing. The chemical composition of aluminum SAE 332 and low-carbon steel discs is presented in **Tables 3** and **4,** respectively.

Table 2. Parameters for the tribological tests.

S/N	Parameter	Value
1	Track radius	5 mm
2	Linear speed	10 cm/s
3	Normal load	8 N
4	Run time	1500 s
5	Linear distance	150 m
6	Acquisition rate	10 Hz
7	Dimension of ball	6 mm
8	Disc diameter	30 mm
9	Temperature	29 ℃
10	Humidity	55%
11	Stop condition	4775 laps

Table 3. Chemical compositions of aluminum SAE 332 disc.

Element	Si	Cu	Mg	Al
% Composition	9.5	3.0	1.0	86.5

Table 4. Chemical compositions of low carbon steel disc.

Element	C	Si	Mn	P	S	Cr	Mo	Ni	Cu	Co	Fe
% Composition	0.105	0.034	1.450	<0.005	<0.127	0.082	0.005	0.208	0.336	0.023	97.757

To identify the phase of the Al_2O_3 nanoparticle samples, the result of the XRD analysis was compared with the positions and intensities of the already known crystallographic structure of the same material.

In the process of characterization of the vegetable oils, the total quantity of NaOH added to the solution to turn it purple-like was observed as recorded as the titer value. The titer value was substituted into Equation (2) to determine the acid value. Half the acid value is the FFA, as shown in Equation (3). The reverse order of this process is used to determine the saponification value. The value of the density was obtained using a specific gravity bottle. The mass and volume of the oil were obtained, and the density was obtained using Equation (4). In the determination of the coefficient of friction (COF), the value of the COF was computed by the InstrumX software based on the principle of Equation (5). This value was recorded for each test carried out. The scar made on the aluminum SAE 332 and low-carbon steel discs represented the wear track for the determination of the wear rate. The diameter of the outer and inner wear tracks is measured. The difference gives the wear volume, which is used to compute the specific wear rate using Equation (6). The size of the diameter is indicative of the lubricant's ability to resist wear. The efficiencies of the nano lubricants were determined by comparing performance and results obtained for the coefficient of friction and the wear rate with the results obtained for the control samples (i.e., samples of vegetable oils at 0% nanoparticle concentration). Equations (7) and (8) were used to ascertain the efficiency of the prepared and tested nano lubricants for the coefficient of friction and wear rate, respectively.

$$\text{Acid value} = \frac{\text{Titer value } \times \text{Concentration of NaOH} \times \text{Molar mass of NaOH}}{\text{Mass of oil}} \tag{2}$$

$$\text{FFA} = \frac{\text{Acid value}}{2} \tag{3}$$

$$\text{Density} = \frac{\text{Mass}}{\text{Volume}} \tag{4}$$

$$\text{COF} = \frac{T\sqrt{6}}{2Wr} \tag{5}$$

$$\text{Specific wear rate} = \frac{\text{Wear volume}}{\text{Load} \times \text{Sliding distance}} \tag{6}$$

$$\varepsilon_{\text{COF}} = \frac{\text{COF}_{\text{CS}} - \text{COF}_{\text{NL}}}{\text{COF}_{\text{CS}}} \times 100\% \tag{7}$$

$$\varepsilon_{\text{WR}} = \frac{\text{WR}_{\text{CS}} - \text{WR}_{\text{NL}}}{\text{WR}_{\text{CS}}} \times 100\% \tag{8}$$

where: T = Frictional torque (kg/mm); W = Applied load (kg), r = Distance from centre of contact surface on the lower ball to the rotation axis (mm), ε_{CoF} = Efficiency of lubricant for coefficient of friction, ε_{WR} = Efficiency of lubricant for wear rate, COF_{NL} = Coefficient of friction of nano lubricant, COF_{CS} = Coefficient of friction of control sample, WR_{NL} = Wear rate of nano lubricant, WR_{CS} = Wear rate of control sample.

3. Results and discussion

The results of the phytochemical screening of plant extract for green synthesis revealed a high presence of tannins, saponins, flavonoids, glycosides, and alkaloids. This is presented in **Table 5**. (++ imply high presence of phytochemicals in the plant extract.) **Figure 3** shows the one-factor graphs, whose plots indicate the effect of each parameter varied on the size of the synthesized Al_2O_3 nanoparticles. The parameters are volume of plant extract (*A*), volume of aqueous solution (*B*), temperature (*C*), speed (*D*), and time (*E*). The graphs show that only volume of the extract and volume of the solution have significant impact on the particle size.

Table 5. Phytochemical screening of *Ipomoea pes-caprae*.

Plant metabolite	Extract content
Tannins	++
Flavonoids	++
Saponins	++
Glycosides	++
Alkaloids	++

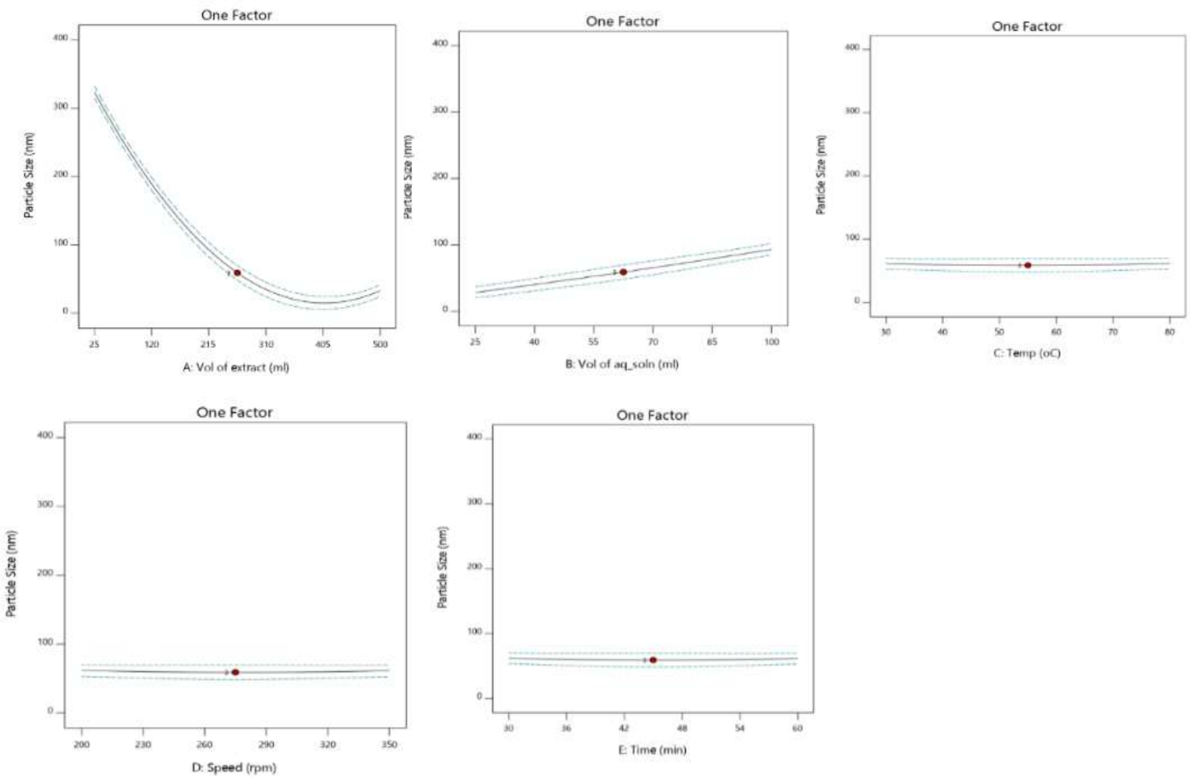

Figure 3. One-factor graphs (A–E).

The result of the UV-Vis analysis is shown in **Figure 4**. A strong and conspicuous absorption peak is observed at 283.00 nm. This confirms the formation of Al_2O_3 nanoparticles in agreement with Selma et al. [15] The result of the nanosizing shows peaks at 9.142 nm, 44.73 nm, and 1210.00 nm corresponding to 10.9% vol, 88.9% vol, and 0.2% vol, respectively, of the synthesized nanoparticles, as shown in **Figure 5**. The result of the nanosizing indicates a close correlation with the predictions from the

DoE using Design Expert software, with the various DoE responses as shown in **Table 6**, which compares the results of the predicted and the actual results of the experiment. The result shows the predicted mean from the DoE to be 44.78 nm, while the experimented mean is 44.73 nm from the nanosizing analysis. A percentage difference of 0.12% was recorded.

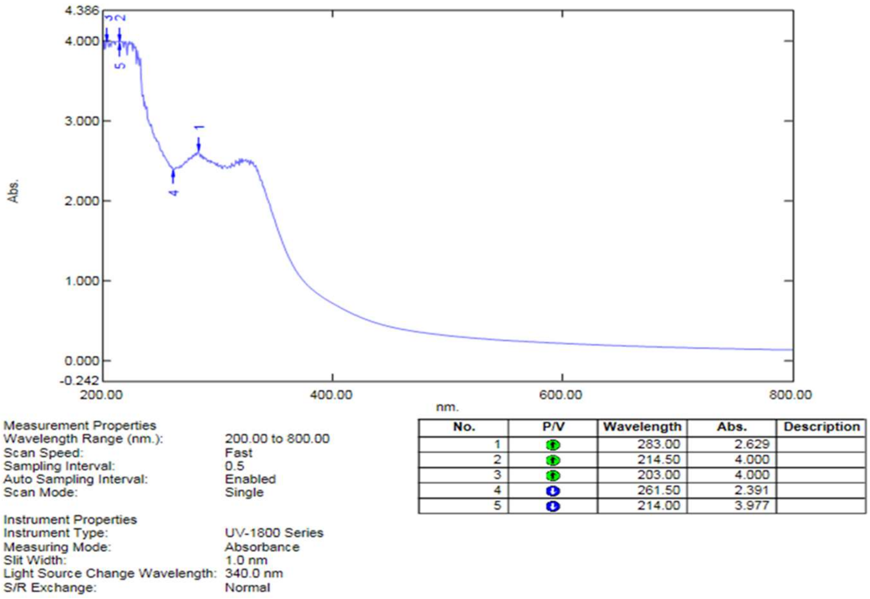

Figure 4. UV-Vis analysis of synthesized Al_2O_3 nanoparticles.

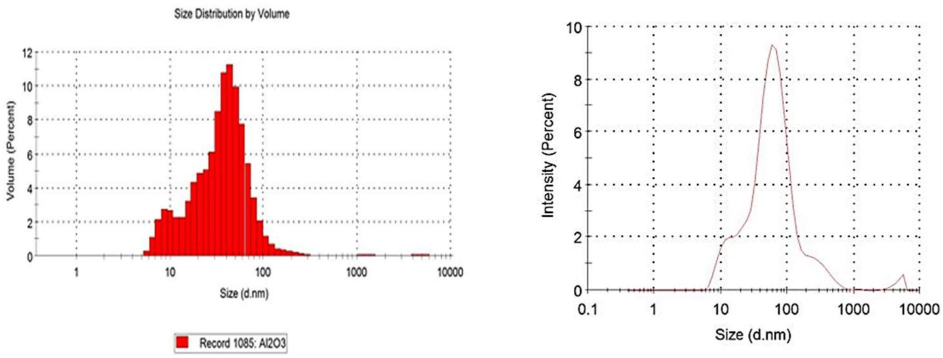

(a) **(b)**

Figure 5. (a) Al_2O_3 nanoparticles size distribution (nanosizing); **(b)** Al_2O_3 nanoparticles size distribution by intensity.

Table 6. Comparison of Predicted and Experimented responses.

Response	Predicted mean	Experimental mean	Difference	% Difference
Particle size	44.784 nm	44.73 nm	0.054	0.12

The characterization of Al_2O_3 nanoparticles through the transmission electron microscopy (TEM) micrographs shows spherically shaped nanoparticles with size distributions of 2 nm as shown in **Figure 6a**, 20 nm in **Figure 6b**, and 50 nm as shown in **Figure 6c**. Furthermore, **Figure 6d** presents the selected area electron diffraction (SEAD), which shows bright continuous diffraction rings, indicating the formation of amorphous Al_2O_3 nanoparticles.

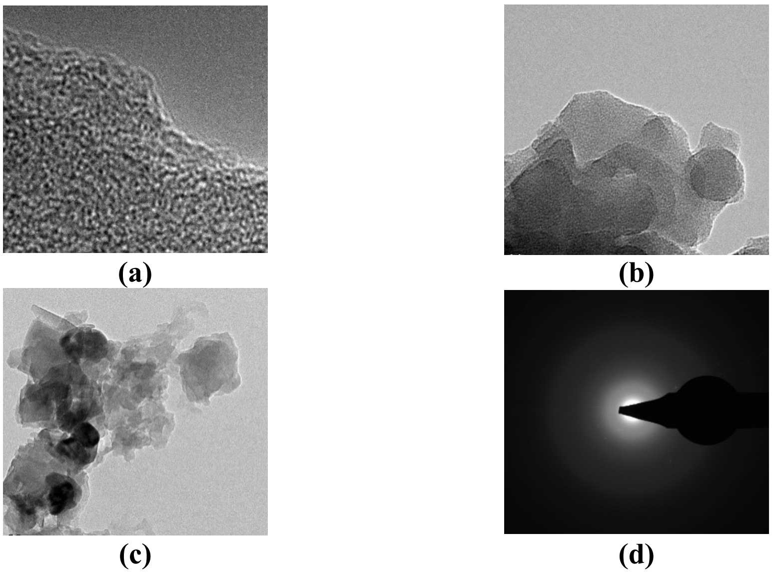

Figure 6. TEM micrographs at **(a)** 2 nm; **(b)** 20 nm; and **(c)** 50 nm; and **(d)** SAED.

Figure 7 shows the X-ray diffraction (XRD) analysis, with observed peaks recorded over a wide range of Bragg angle 2θ (20° ≤ 2θ ≤ 80°). This confirmed the formation of Al_2O_3 nanoparticles by the transformation of Al to Al_2O_3 using $Al(NO_3)_3$ salt as precursor and *Ipomoea pes-caprae* plant extract as reducing agent. The results of the tribological test for COF of the nano lubricants on low-carbon steel and aluminum SAE 332 discs are presented in **Figures 8–10**. All nano lubricants of castor oil, jatropha oil and PKO have significantly lower COF on aluminum SAE 332 discs compared to PKO without Al_2O_3 nanoparticles. **Figure 8** (L) shows that nano lubricants with 0.5 wt% and 1.0 wt% have significantly lower COF on aluminum SAE 332 discs compared to castor oil without Al_2O_3 nanoparticles.

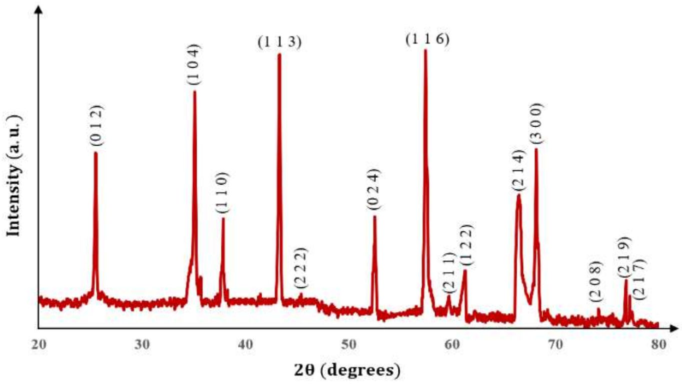

Figure 7. XRD Pattern of Al_2O_3 NPs using *Ipomoea pes-caprae* extract.

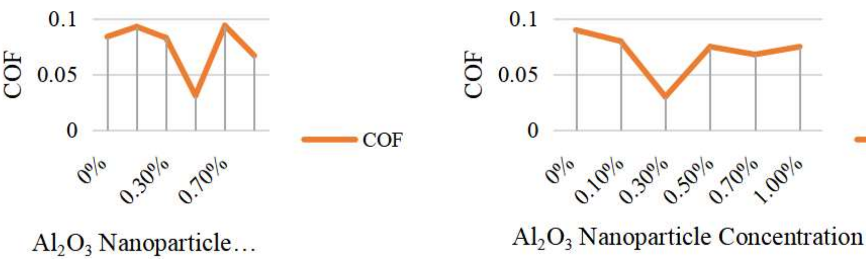

Figure 8. COF of castor oil (L) and jatropha oil (R) on aluminum SAE 332 discs.

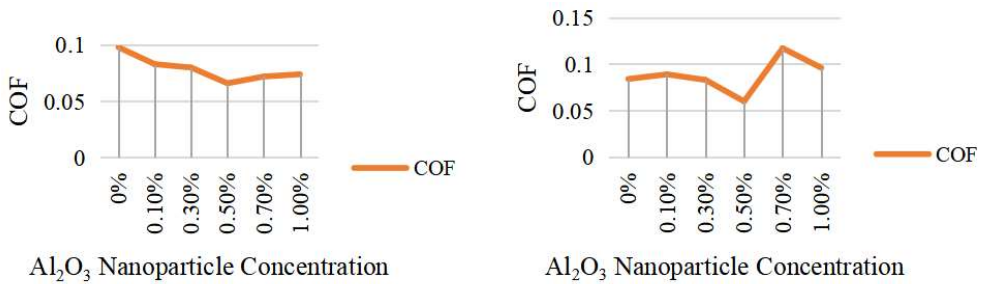

Figure 9. COF of Palm kernel oil on aluminum SAE 332 discs (L) and COF of castor oil on Low carbon steel disc (R).

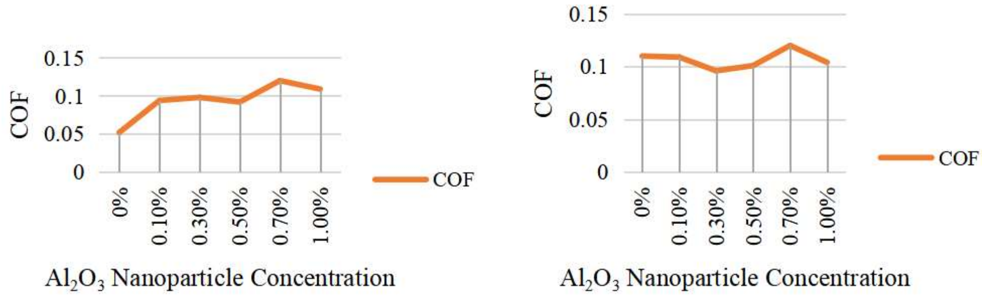

Figure 10. COF of jatropha oil on low carbon steel disc (L) and COF of PKO on low carbon steel disc (R).

Figure 8 (R) shows that nano lubricant with 0.3 wt% Al_2O_3 nanoparticles concentration gave the most desirable result with COF of 0.030 against a COF of 0.090 at 0 wt% concentration.

Figure 9 (L) shows that nano lubricant with 0.5 wt% Al_2O_3 nanoparticles concentration gave the most desirable result with COF of 0.066 against a COF of 0.098 at 0 wt% concentration and **Figure 8** (R) shows a significantly lower COF was observed at 0.5 wt% Al_2O_3 nanoparticles, beyond which the nano lubricant demonstrated higher COF compared to castor oil at 0 wt% Al_2O_3 nanoparticles.

Figure 10 (L) shows that the nano lubricants demonstrated significantly higher COF compared to jatropha oil without Al_2O_3 nanoparticles, making jatropha oil demonstrate better performance in inhibiting friction on low-carbon steel discs compared to samples with Al_2O_3 nanoparticle additives. **Figure 9** (R) shows nano lubricant with 0.3 wt% demonstrated significantly lower COF on low-carbon steel discs compared to castor oil without Al_2O_3 nanoparticles. The results of the tribological test for wear rate of the nano lubricants on low-carbon steel and aluminum SAE 332 discs are presented in **Figures 11–13**.

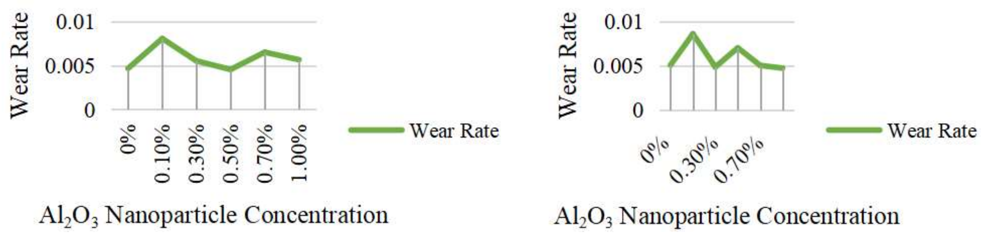

Figure 11. Wear rate of castor oil (L) and jatropha oil (R) on aluminium SAE 332 discs.

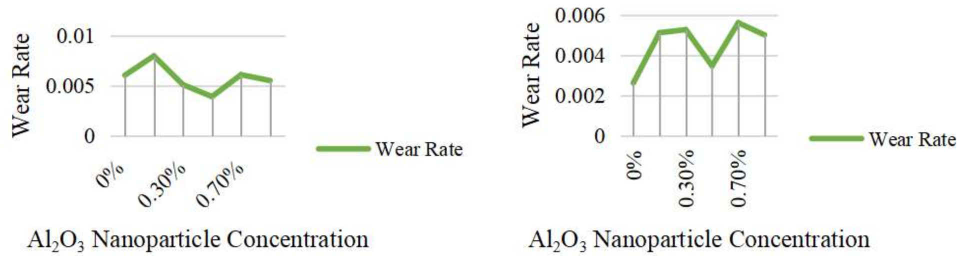

Figure 12. Wear rate of palm kernel oil on aluminium SAE 332 discs (L) and wear rate of castor oil on low carbon disc (R).

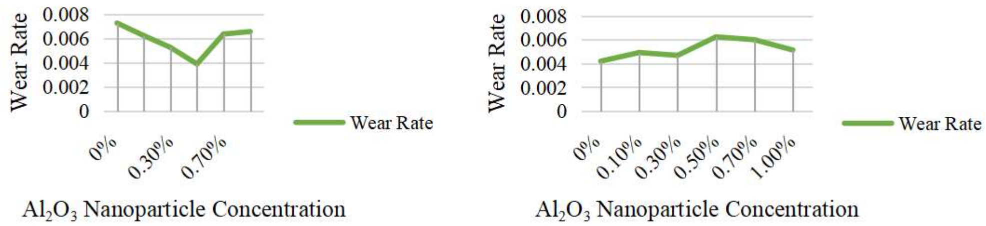

Figure 13. Wear rate of jatropha oil (L) and palm kernel oil (R) on low carbon steel disc.

Figure 11 (L) shows that the nano lubricant with 0.5 wt% demonstrated a slightly lower wear rate on aluminum SAE 332 discs compared to castor oil without Al_2O_3 nanoparticles. **Figure 11** (R) shows that the addition of Al_2O_3 nanoparticles at 0.1 wt% and 0.5 wt% concentrations significantly increased the wear rate, and the nano lubricant with 1.0 wt% Al_2O_3 nanoparticle concentration demonstrated a wear rate of 0.004727 $mm^3N^{-1}m^{-1}$, compared to the wear rate of 0.005064 $mm^3N^{-1}m^{-1}$ at 0 wt% concentration.

Figure 12 (L) shows that nano lubricant with a 0.5 wt% Al_2O_3 nanoparticle concentration gave the most desirable result with a wear rate of 0.003915 $mm^3N^{-1}m^{-1}$, compared to a wear rate of 0.006037 $mm^3N^{-1}m^{-1}$ at a 0 wt% concentration. **Figure 12** (R) shows that all nano lubricant formulated demonstrated a higher wear rate compared to castor oil without Al_2O_3 nanoparticles, with a wear rate of 0.002627 $mm^3N^{-1}m^{-1}$.

Figure 13 (L) shows a steady reduction in wear rate upon addition of Al_2O_3 nanoparticles to jatropha oil was observed from 0.1 wt% to 0.5 wt%, demonstrating the lowest wear rate. **Figure 13** (R) shows that all nano lubricant formulated demonstrated a higher wear rate compared to castor oil without Al_2O_3 nanoparticles with a wear rate of 0.004191 $mm^3N^{-1}m^{-1}$. On the efficiency of the base oils and nano lubricants, the efficiency of castor oil, jatropha oil, and PKO with nano lubricants on COF on aluminum SAE 332 discs has the nano lubricant with 0.5 wt% Al_2O_3 nanoparticles had the highest efficiency with 92.29%, 0.3 wt% Al_2O_3 nanoparticles recorded the highest efficiency of 92.54% and 0.5 wt% Al_2O_3 nanoparticles recorded the highest efficiency of 83.58%, respectively. The computation of the efficiency of oils and the nano lubricants with castor oil, jatropha oil, and PKO as base oils on COF using a low-carbon steel disc has the nano lubricant with 0.5 wt% Al_2O_3 nanoparticles recording the highest efficiency of 87.80%, while jatropha oil without Al_2O_3 nanoparticle additives recorded the highest efficiency of 89.43%, with the closest nano lubricant recording an efficiency of 81.30 at 0.5 wt% Al_2O_3 nanoparticle concentration and the nano lubricant with 0.3 wt% Al_2O_3 nanoparticles recorded the highest efficiency of 80.49% for PKO. The computation of the efficiency of castor oil, jatropha oil, and PKO and the nano lubricants with the oils as base oils on wear rate using aluminum SAE 332 discs has the nano lubricant with 0.5 wt% Al_2O_3 nanoparticles had the highest efficiency with 76.20% for the castor oil, while the nano lubricant with 1.0 wt% Al_2O_3 nanoparticles recorded the highest efficiency of 75.29% jatropha oil and the nano lubricant with 0.5 wt% Al_2O_3 nanoparticles recorded the highest efficiency of 79.53% for PKO. The computation of the efficiency of the oils and the nano lubricants with castor oil without Al_2O_3 nanoparticle additive recorded the highest efficiency of 64.65%, while jatropha oil with 0.5 wt% Al_2O_3 nanoparticle concentration recorded the highest efficiency of 47.65%, and for PKO, all nano lubricant had lower efficiency compared to PKO without Al_2O_3 nanoparticle additives with an efficiency of 43.61%.

4. Conclusion

Al_2O_3-castor oil nano lubricant significantly reduced COF on aluminum SAE 332 and low-carbon steel from 0.084 without Al_2O_3 nanoparticles to 0.031 and from 0.084 to 0.060 at 0.5 wt%, respectively. Al_2O_3—jatropha nano lubricant reduced COF on aluminum SAE 332 from 0.090 without Al_2O_3 nanoparticles to 0.030 when Al_2O_3 nanoparticles were added at 0.3 wt%. On low-carbon steel, an increase in COF was recorded across all concentrations of Al_2O_3 nanoparticles. Similarly, Al_2O_3—palm kernel oil on aluminum SAE 332 demonstrated a reduction in COF from 0.098 to 0.066 at concentrations of 0.5 wt%. On low-carbon steel, the COF mostly increased. The test for the wear rate of Al_2O_3—castor nano lubricant indicated an increase in wear rate on aluminum SAE 332 and low-carbon steel. Similarly, Al_2O_3—jatropha nano lubricant on aluminum SAE 332 demonstrated an increase in wear rate. However, on low-carbon steel, the wear rate reduced from 0.007265 without Al_2O_3 nanoparticles to 0.003891 at 0.5 wt% Al_2O_3 nanoparticle additives. Al_2O_3—PKO nano lubricant on aluminum SAE 332 demonstrated a reduction in wear rate from 0.006037 without Al_2O_3 nanoparticles to 0.003915 at 0.5 wt% of Al_2O_3 nanoparticles. On low-carbon steel, however, the wear rates increased across all concentrations.

Author contributions: Conceptualization, SYT, TJO and SAL; methodology, SYT, and TJO; software, UGO; validation, JA, IOS and EOO; formal analysis, DIT and AAA; investigation, AS and EAK; resources, SAL; data curation, SAL and UGO; writing—original draft preparation, SYT; writing—review and editing, SAL and UGO; visualization, JA; supervision, SAL and TJO; project administration, SAL; funding acquisition, SYT and SAL. All authors have read and agreed to the published version of the manuscript.

Conflict of interest: The authors declare no conflict of interest.

References

1. Dai W, Kheireddin B, Gao H, et al. Roles of nanoparticles in oil lubrication. Tribology International. 2016; 102: 88-98. doi: 10.1016/j.triboint.2016.05.020

2. Ghaednia H, Hossain MS, Jackson RL. Tribological Performance of Silver Nanoparticle–Enhanced Polyethylene Glycol Lubricants. Tribology Transactions. 2016; 59(4): 585-592. doi: 10.1080/10402004.2015.1092623
3. Hwang Y, Lee JK, Lee JK, et al. Production and dispersion stability of nanoparticles in nanofluids. Powder Technology. 2008; 186(2): 145-153. doi: 10.1016/j.powtec.2007.11.020
4. Mohan D, Pittman CU, Bricka M, et al. Sorption of arsenic, cadmium, and lead by chars produced from fast pyrolysis of wood and bark during bio-oil production. Journal of Colloid and Interface Science. 2007; 310(1): 57-73. doi: 10.1016/j.jcis.2007.01.020
5. Lawal SA, Choudhury IA, Nukman Y. Application of vegetable oil-based metalworking fluids in machining ferrous metals—A review. International Journal of Machine Tools and Manufacture. 2012; 52(1): 1-12. doi: 10.1016/j.ijmachtools.2011.09.003
6. Salimon J, Abdullah BM, Salih N. Saponification of Jatropha curcas Seed Oil: Optimization by D-Optimal Design. International Journal of Chemical Engineering. 2012; 2012: 1-6. doi: 10.1155/2012/574780
7. Mahesar SA, Sherazi STH, Khaskheli AR, et al. Analytical approaches for the assessment of free fatty acids in oils and fats. Anal Methods. 2014; 6(14): 4956-4963. doi: 10.1039/c4ay00344f
8. Jeevanandam J, Barhoum A, Chan YS, et al. Review on nanoparticles and nanostructured materials: history, sources, toxicity and regulations. Beilstein Journal of Nanotechnology. 2018; 9: 1050-1074. doi: 10.3762/bjnano.9.98
9. Griffis C, Wilson T, Schneider J, Pierpont P. Unmanned Aircraft System Propulsion Systems Technology Survey. Available online: https://commons.erau.edu/cgi/viewcontent.cgi?article=1042&context=publication (accessed on 2 January 2024).
10. Trofymov I, Svyryd M, Matveyeva O, Sydorenko O. Influence of electromagnetic treatment of fuels and oils on the formation of wear resistance of friction pairs. In: Selected Aspects of Providing the Chemmotological Reliability of the Engineering. National Aviation University; 2019. pp. 141-153. doi: 10.18372/38236
11. Dai C, Zhang A, Liu M, et al. Hollow Alveolus-Like Nanovesicle Assembly with Metal-Encapsulated Hollow Zeolite Nanocrystals. ACS Nano. 2016; 10(8): 7401-7408. doi: 10.1021/acsnano.6b00888
12. Kart HH, Yildirim H, Ozdemir Kart S, et al. Physical properties of Cu nanoparticles: A molecular dynamics study. Materials Chemistry and Physics. 2014; 147(1-2): 204-212. doi: 10.1016/j.matchemphys.2014.04.030
13. Rastogi A, Zivcak M, Sytar O, et al. Impact of Metal and Metal Oxide Nanoparticles on Plant: A Critical Review. Frontiers in Chemistry. 2017; 5. doi: 10.3389/fchem.2017.00078
14. NadaroĞLu H, Güngör AA, Nce S. Synthesis of Nanoparticles by Green Synthesis Method Synthesis of Nanoparticles by Green Synthesis Method. International Journal of Innovative Research and Reviews. 2017; 1(1): 6-9.
15. Selma MA, Sarya DMA, Wafaa KK. Characterization of Laser Ablated Nanostructured Al_2O_3/p-Solar Cells. Iraqi Journal of Applied Physics. 2015; 11(1): 29-32.

Appendix

Figure A1. Graphical abstract.